

Super-resolution image restoration algorithm based on orthogonal discrete wavelet transform

Yangyang Liu (刘扬阳), Weiqi Jin (金伟其), and Binghua Su (苏秉华)

Department of Optical Engineering, School of Information Science Technology,
Beijing Institute of Technology, Beijing 100081

Received April 30, 2004

By using orthogonal discrete wavelet transform (ODWT) and generalized cross validation (GCV), and combining with Luck-Richardson algorithm based on Poisson-Markov model (MPML), several new super-resolution image restoration algorithms are proposed. According to simulation experiments for practical images, all the proposed algorithms could retain image details better than MPML, and be more suitable to low signal-to-noise ratio (SNR) images. The single operation wavelet MPML (SW-MPML) algorithm and MPML algorithm based on single operation wavelet transform (MPML-SW) avoid the iterative operation of self-adaptive parameter in MPML particularly, and improve operating speed and precision. They are instantaneous to super-resolution image restoration process and have extensive application foreground.

OCIS codes: 100.6640, 100.3010, 100.7410.

Recently, super-resolution image restoration theory develops rapidly. If the image degradation process is not reversible, super-resolution image restoration algorithms might use *a priori* limited degradation parameter, under the condition that the low frequency information in frequency-pass bands can be restored, to restore blurred images by restoring high frequencies beyond the cut-off frequency. Therefore image details can be retrieved so much that the restored image is greatly close to the original object^[1,2]. It is practical to image reconstruction.

Poisson-Luck-Richardson super-resolution image restoration algorithm with Markov constraint (MPML) based on Bayes statistical analysis theory supposes that the image has Poisson and Markov distributions and adopts maximum-likelihood theory to estimate blurred image, which can be express as^[3]

$$f_{ij}^{n+1} = f_{ij}^n \left[\left(\frac{g_{ij}}{(h * f^n)_{ij}} \right) \oplus h_{ij} - \alpha \frac{\partial}{\partial f_{ij}} U(f^n) \right]^p, \quad (1)$$

where g is the degradation image, h is a point spread function of imaging system, $*$ is a convolution operator, n is the order number of iterative, \oplus is a correlation operator, $U(f)$ is the energy function in Gibbs distribution, namely Markov constraint, α is the regularization self-adaptive parameter adjusted synchronously with every iterative step, K_1 and K_2 are two step-controlling coefficients which could be confirmed only by the respective input measured image^[3] and implement its self-adaptive process for constraining weight unbalance part in iterative process, and p is a controlling coefficient to control the algorithm's convergence and iterative speed. The algorithm has used *a priori* information for the object and is applicable to linear and nonlinear imaging models with a unique solution when noise is not severe. But the restoration process may produce some ringing fringes, and the restored results are not ideal for high frequency loss and distortion in relatively noisy images. Therefore the images with ordinary signal-to-noise ratio (SNR) of 10–20 could not be recovered well by the algorithm in practice.

The orthogonal discrete wavelet transform (ODWT) has the capability of indicating local features of a signal and concentrating the signal power to a few coefficients in wavelet transform domain. It is introduced here and combined with MPML to resolve the problem of low SNR image restoration.

The degradation discrete images are

$$g(i, j) = h(i, j) * f(i, j) + \varepsilon(i, j) \quad (i, j = 1, \dots, N), \quad (2)$$

where $f(i, j)$ is the original image, ε is noise, (x, y) are two-dimensional (2D) variables in space domain.

By Eq. (1), MPML is updated as

$$f(i, j)^{n+1} = f(i, j)^n \left[\left(\frac{h(i, j) * f(i, j) + \varepsilon(i, j)}{h(i, j) * f(i, j)^n} \right) \oplus h(i, j) - \alpha \frac{\partial}{\partial f_{ij}} U(f^n) \right]^p. \quad (3)$$

Assume that ε is a stationary stochastic uncorrelated noise with zero mean and variance σ^2 . Equation (2) can be expressed with ODWT^[4] as

$$Y = X + V, \quad (4)$$

where $X = W[h * f]$, $V = W[\varepsilon]$, $Y = W[g]$, and W is a 2D orthogonal wavelet transform matrix.

According to different characteristics of respective high frequency subbands, a suitable threshold δ can be chosen to resolve the existed available signal remove or reduce noise influence on image. Thus the noise effect in MPML may be reduced.

A thresholding operation T_δ to wavelet transformed image Y yields

$$Y_\delta = T_\delta[Y]. \quad (5)$$

All inverse wavelet transform can be given as

$$g_\delta = W^{-1}[Y_\delta] = W^{-1}\{T_\delta[W[g]]\}. \quad (6)$$

The new algorithm from updated MPML is the algorithm of MPML operation after wavelet transform (W-MPML) and the algorithm of MPML operation before wavelet transform (MPML-W). For W-MPML,

$$f_{ij}^{n+1} = f_{ij}^n \left[\left(\frac{g_\delta}{(h * f^n)_{ij}} \right) \oplus h_{ij} - \alpha \frac{\partial}{\partial f_{ij}} U(f^n) \right]^p, \quad (7)$$

and for MPML-W,

$$f_{ij}^{n+1} = \left\{ f_{ij}^n \left[\left(\frac{g_{ij}}{(h * f^n)_{ij}} \right) \oplus h_{ij} - \alpha \frac{\partial}{\partial f_{ij}} U(f^n) \right]^p \right\}_\delta. \quad (8)$$

According to simulating experiments for practical images, the restoration results and evaluating parameters of MPML-W and W-MPML are obviously better than those of MPML itself, but the degraded images are still recovered poorly.

From the physics meaning, referring to lower SNR (larger noise) problem, the restriction from the regulation parameter α and wavelet transform is destroyed by too much iterative in W-MPML and MPML-W, which can also be seen in practical experiments. Whereas W-MPML and MPML-W did not begin iterative operation, namely when n in Eqs. (7) and (8) equals 1, the constraint factors reach the optimal matching to each other. So the restoration results are better than degradation and restored images by W-MPML and MPML-W algorithms, and even operation time is much fewer than that of W-MPML and MPML-W. The mean square error (MSE) values of the reconstructed images by W-MPML and MPML-W along with iterative times are presented in Figs. 1 and 2.

Therefore the single operation of W-MPML and MPML-W algorithms is further proposed, for the single operation of W-MPML algorithm, the restored image can

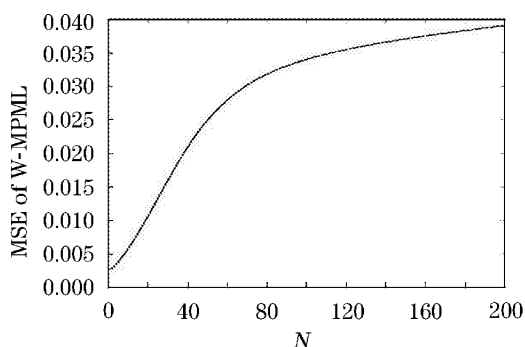


Fig. 1. The MSE value of the reconstructed image by W-MPML along with iterative times N .

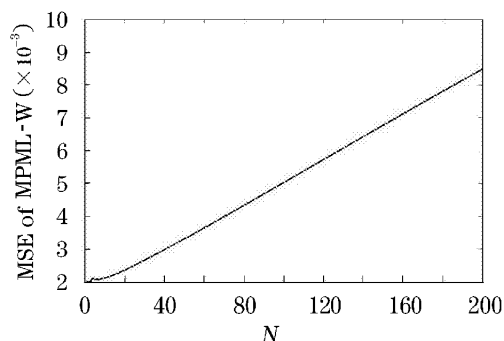


Fig. 2. The MSE value of the reconstructed image by MPML-W along with iterative times N .

be expressed as

$$\hat{f}_{ij} = g_\delta \left[\left(\frac{g_\delta}{(h * f)_{ij}} \right) \oplus h_{ij} - \alpha \frac{\partial}{\partial f_{ij}} U(g_\delta) \right]^p, \quad (9)$$

and for the single operation of MPML-W algorithm,

$$\hat{f}_{ij} = \left\{ f_{ij} \left[\left(\frac{g_{ij}}{(h * g)_{ij}} \right) \oplus h_{ij} - \alpha \frac{\partial}{\partial f_{ij}} U(g) \right]^p \right\}_\delta. \quad (10)$$

The SW-MPML and MPML-SW algorithms give attention to the de-blurring advantages, and extract the energy function under Markov distribution in MPML. At the same time, they utilize more superior de-noising capability of ODWT instead of α , with timesaving α as one constant fit of common to omit iterative process and even time. The SW-MPML and MPML-SW algorithms are instantaneous under 10–20 dB of the low SNR image restoration project.

However the validity of SW-MPML and MPML-SW is decided by the optimal threshold δ in the respective high frequency subbands, so how to choose the optimal threshold δ is the key for the new proposed algorithms.

It is difficult for practical application to use the MSE function and other more complex parameters in evaluating the optimal threshold δ , so the generalized cross validation (GCV) theory is introduced to resolve this problem here^[5,6].

According to the proposed soft-threshold in Ref. [6], the updated new matrix T_δ is

$$Y_\delta(i, j) = T_\delta N[Y] = \begin{cases} 0 & |Y(i, j)| < \delta \\ Y(i, j) - \delta & |Y(i, j)| \geq \delta \end{cases} \quad (i, j = 1, \dots, N). \quad (11)$$

The cells $t'(m, n)$ of the threshold derivative matrix T' could be represented as

$$t'(m, n) = \frac{\partial Y_\delta(i, j)}{\partial Y(k, l)} = \begin{cases} 0 & m \neq n \\ \begin{cases} 0 & |Y(i, j)| < \delta \\ 1 & |Y(i, j)| \geq \delta \end{cases} & m = n \end{cases}, \quad (12)$$

where $k, l=1, \dots, N$, $m = (i-1)N + j$, and $n = (k-1)N + l$.

An asymptotically optimal threshold is determined by minimizing GCV, which is based on ordinary cross validation (OCV) and aimed at an unknown exact signal^[6]. Assume that \tilde{Y}_i is a neighbours' combination of Y_i ($i=1, \dots, N^2$), not including Y_i itself, such as $\tilde{Y}_i = \frac{1}{2}(Y_{i-1} + Y_{i+1})$, an optimal combination \tilde{Y}_i to minimize noise is possible. Similarly, assume that $\tilde{Y}_{\delta i}$ is a neighbours' combination of $Y_{\delta i}$ ($i=1, \dots, N^2$), then $\tilde{Y}_{\delta i} = \tilde{Y}_i$ will turn out to be an interesting choice. OCV is

$$\text{OCV}(\delta) = \frac{1}{N^2} \sum_{i,j=1}^N [Y(i, j) - \tilde{Y}_\delta(i, j)]^2. \quad (13)$$

For too small values of δ , the difference $Y(i, j) - \tilde{Y}_\delta(i, j)$ is dominated by noise, while for large values of δ , the signal itself is distorted too much. So δ of the minimized

OCV corresponds to the best compromise between image fitting and smoothness.

Equation (13) is transformed because of unidentified \tilde{Y}_δ under unknown δ ^[5], so OCV is represented as

$$OCV(\delta) \approx \frac{1}{N^2} \sum_{i,j=1}^N \sum_{m=1}^{N^2} \frac{[Y(i,j) - Y_\delta(i,j)]^2}{[1 - t'(m,n)]^2}. \quad (14)$$

However it cannot be used in practical computations, since $t'(m,m)$ is 0 or 1. Therefore some kinds of mean values for $[1 - t'(m,n)]$ are taken, the so-called GCV^[5] is given as

$$WGCV(\delta) = \frac{\frac{1}{N^2} \cdot \|Y - Y_\delta\|^2}{\left[\frac{\text{trace}(I - T')}{N^2}\right]^2}. \quad (15)$$

If $\delta^* = \arg \min \text{MSE}(\delta)$ and $\tilde{\delta} = \arg \min \text{GCV}(\delta)$, Ref. [5] proves that, for $N \rightarrow \infty$, both minimizers yield a result of the same quality as

$$\frac{\text{EMSE}(\tilde{\delta})}{\text{EMSE}(\delta^*)} \rightarrow 1, \quad (16)$$

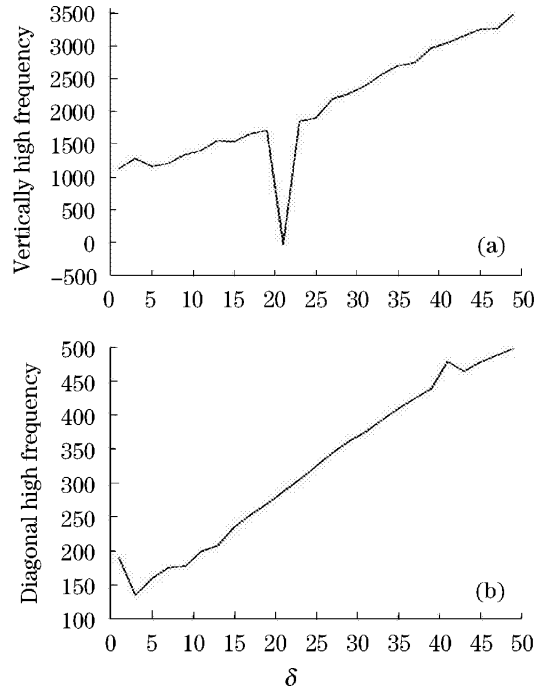


Fig. 3. The curves of WGCV with δ . (a): Vertically high frequency; (b): diagonal high frequency.



Fig. 4. “Lena” restorations. (a): Original image ($N = 256$); (b): noisy image (SNR = 10 dB); (c): restored SNR = 30 image by MPML; (d): restored by MPML; (e): restored by W-MPML; (f): restored by MPML-W; (g): restored by SW-MPML; (h): restored by MPML-SW.

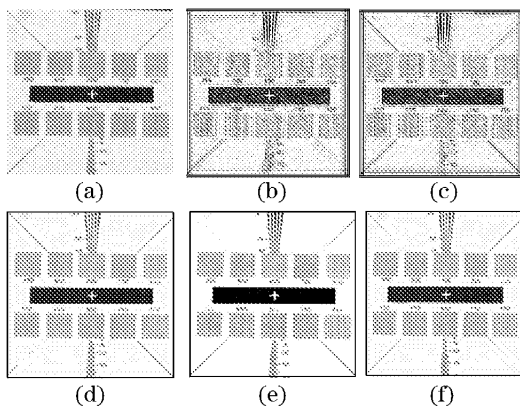


Fig. 5. Restoration of “part” images. (a): Original image of part chart; (b): restored by MPML; (c): restored by W-MPML; (d): restored by MPML-W; (e): restored by SW-MPML; (f): restored by MPML-SW.

it is the reason that the δ obtained from GCV is asymptotically optimal. As for the estimating solution process of δ , the value range of δ is positive value in wavelet decomposition coefficients, namely the value range of Y , with the WGCV computation results as Fig. 3, and δ does not need to be computed exactly. So the stationary point δ corresponding to the minimized $\text{WGCV}(\delta)$ is chosen as optimal δ .

The closeness of restoration to original image is evaluated by MSE, peak SNR (PSNR), and the improved SNR (ISNR). A 256×256 “Lena” image (SNR = 20) is restored as Fig. 4, where MPML reconstructing advantage is presented as Fig. 4(c) when SNR is 30. And a part (SNR = 20) of “Test Charts of Reflection for Television Multiple Test Chart (GB/T13170.1-91)” captured in experiment is restored as Fig. 5.

A comparison among MSE, PSNR, and ISNR is shown in Table 1.

Table 1. The Evaluating Values of MSE, PSNR, and ISNR for Two Images by Different Algorithms

Image	SNR (dB)	Algorithm	MSE	PSNR	ISNR
Lena	20	Degradation Image	0.0092	20.3621	
		MPML	0.2353	6.2838	-14.0783
		W-MPML	0.1010	9.9568	-10.4053
		MPML-W	0.0105	19.7881	-0.5740
		SW-MPML	0.0090	20.4576	0.0955
		MPML- SW	0.0102	19.9140	-0.4481
Part	20	Degradation Image			
		MPML	0.2819	5.4990	
		W-MPML	0.2787	5.5486	
		MPML-W	0.0062	22.0761	
		SW-MPML	0.0056	22.5181	
		MPML- SW	0.0062	22.0761	

To seek a way for resolving image restoration problem under lower SNR, W-MPML, MPML-W, and the single operation of the W-MPML and MPML-W algorithms are proposed. After the degradation image is "Symlets" wavelet transformed, an asymptotically optimal threshold is determined by minimizing GCV theory, and high frequency subbands in each decomposition level are denoised with soft threshold processes to converge respectively to those with maximum SNR, when the method is incorporated with the existing MPML, details of original image, especially those with low SNR could be well recovered. SW-MPML and MPML-SW are some operative algorithms proposed based on the method. According to the processing results of the simulating and practical images, in comparison with MPML, because of only one operation, under the guarantee of rapid and effective processing, they could also remove iterative operation time for up to hundreds times, as well as avoid the iterative operation of self-adaptive parameters in MPML, improve

operating speed and precision. They are practical and instantaneous to the low SNR image restoration.

Y. Liu's e-mail address is liuyangyang01@bit.edu.cn.

References

1. B. H. Su, *Investigation of Image Super-Resolution Restoration* (in Chinese) Ph.D thesis (Beijing Institute of Technology, 2002) p.1.
2. B. H. Su and W. Q. Jin, *Acta Photon. Sin.* (in Chinese) **32**, 502 (2003).
3. B. H. Su and W. Q. Jin, *Acta Electron. Sin.* (in Chinese) **31**, 41 (2003).
4. S. G. Mallat, *IEEE Trans. Pattern Analysis and Machine Intelligence* **11**, 674 (1989).
5. M. Jansen, M. Malfait, and A. Bultheel, *Signal Processing* **56**, 33 (1997).
6. D. L. Donoho, *IEEE Trans. Information Theory* **41**, 613 (1995).